

AB

RECENT RESULTS FROM THE CCFR NEUTRINO  
EXPERIMENT AT THE TEVATRON

W.H. Smith, T. Kinnel, P.H. Sandler

*Physics Department, University of Wisconsin, Madison, WI 53706 USA*

C.G. Arroyo, K.T. Bachmann, A.O. Bazarko, T. Bolton, C. Foudas, B.J. King,  
W.C. Lefmann, W.C. Leung, S.R. Mishra, E. Oltman, P.Z. Quintas,  
S.A. Rabinowitz, F.J. Sciulli, W.G. Seligman, M.H. Shaevitz

*Physics Department, Columbia University, New York, NY 10027 USA*

F.S. Merritt, M.J. Oreglia, B.A. Schumm

*Physics Department, University of Chicago, Chicago, IL 60637 USA*

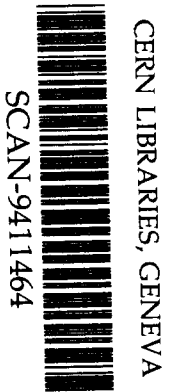
R.H. Bernstein, F. Borcharding, H.E. Fisk, M.J. Lamm, W. Marsh,  
K.W.B. Merritt, H.M. Schellman, D.D. Yovanovitch

*Physics Division, Fermilab, Batavia, IL 60510 USA*

A. Bodek, H.S. Budd, P. de Barbaro, W.K. Sakumoto,

*Physics Department, University of Rochester, Rochester, NY 14627 USA*

92 3449



ABSTRACT

We present the first next-to-leading-order QCD analysis of neutrino charm production, using a sample of 6090  $\nu_\mu$ - and  $\bar{\nu}_\mu$ -induced events gathered with the CCFR detector at the Fermilab Tevatron. We find that the nucleon strange quark content is suppressed with respect to the non-strange sea quarks by a factor  $\kappa = 0.477^{+0.063}_{-0.053}$ , the strange sea  $x$ -dependence is similar to that of the non-strange sea, and that the measured charm quark mass,  $m_c = 1.70 \pm 0.19 \text{ GeV}/c^2$ . Further analysis finds that the difference in  $x$ -distributions between  $xs(x)$  and  $x\bar{s}(x)$  is small. We also measure the Cabibbo-Kobayashi-Maskawa matrix element  $|V_{cd}| = 0.232^{+0.018}_{-0.020}$ .

1. Data Sample

The dimuon data were accumulated during two runs, E744 and E770, with the Chicago-Columbia-Fermilab-Rochester (CCFR) detector, using the Fermilab Tevatron Quadrupole-Triplet neutrino beam with energies up to 600 GeV. In the CCFR detector,<sup>1</sup> neutrino interactions occur in the 690 ton unmagnetized steel-scintillator target-calorimeter, which is instrumented with drift chambers for muon tracking and followed by a solid-iron toroidal magnetic spectrometer, which identifies muons and measures their momenta.

Charged-current single muon events are required to have  $E_{\text{vis}} > 30$  GeV,  $E_{\text{had}}^{\text{vis}} > 10$  GeV,  $Q_{\text{vis}}^2 > 1$  GeV<sup>2</sup>/c<sup>2</sup> and  $p_{\mu_1} > 9$  GeV/c, where  $E_{\text{vis}} = E_{\mu_1} + E_{\mu_2} + E_{\text{had}}^{\text{vis}}$  and  $Q_{\text{vis}}^2 = 4E_{\text{vis}}E_{\mu_1}\sin^2(\theta_{\mu_1}/2)$ . Dimuon events are selected by making the further requirement that the second muon has  $p_{\mu_2} > 5$  GeV/c and that both muons have  $\theta_{\mu} < 0.250$  rad. The second muon's momentum is measured in the magnetic spectrometer whenever possible, otherwise it is determined from the muon's range in the target. In order to reduce non-prompt sources of second muons, events in which muon 2 does not reach the toroid must also satisfy  $E_{\text{had}}^{\text{vis}} < 130$  GeV. The final dimuon sample contains 6090 events. Results from a leading-order analysis of this data sample were reported previously.<sup>2</sup>

## 2. Differential cross section

At leading order (LO) charm is produced by scattering directly off strange and down quarks in the nucleon. The LO differential cross section for an isoscalar target, neglecting target mass effects, is given by:

$$\left\{ \frac{d^2\sigma(\nu_{\mu}N \rightarrow cX)}{d\xi dy} \right\}_{LO} = \frac{G^2 M E_{\nu}}{\pi(1 + Q^2/M_W^2)^2} \{ [\xi u(\xi, \mu^2) + \xi d(\xi, \mu^2)] |V_{cd}|^2 + 2\xi s(\xi, \mu^2) |V_{cs}|^2 \} \left( 1 - \frac{m_c^2}{2ME_{\nu}\xi} \right), \quad (1)$$

where  $\xi u(\xi, \mu^2)$ ,  $\xi d(\xi, \mu^2)$  and  $\xi s(\xi, \mu^2)$  represent the momentum distributions of the  $u$ ,  $d$  and  $s$  quarks within the proton (the corresponding  $\bar{\nu}_{\mu}$  process has the quarks replaced by their antiquark partners) and  $|V_{cd}|$  and  $|V_{cs}|$  are the CKM matrix elements. The mass of the charm quark,  $m_c$  introduces an energy threshold in the charm production rate. Neglecting the small effect of the initial state quark mass,  $\xi$ , the momentum fraction of the struck quark, is related to the Bjorken scaling variable  $x$  by slow-rescaling<sup>4</sup>:

$$\xi = x \left( 1 + \frac{m_c^2}{Q^2} \right) \left( 1 - \frac{x^2 M^2}{Q^2} \right). \quad (2)$$

## 3. Analysis

The charm-induced dimuon generator simulates the production of  $D$  mesons. The species of charmed particles produced in neutrino interactions as a function of neutrino energy was measured by Fermilab E531,<sup>5</sup> and for  $E_{\nu} > 30$  GeV is dominated by charged and neutral  $D$  mesons. Fragmentation to  $D$ 's in the Monte Carlo simulation is parameterized by the fragmentation function of Collins and Spiller,<sup>6</sup>  $D(z) = N [(1-z)/z + \epsilon(2-z)/(1-z)](1+z)^2 [1 - (1/z) - \epsilon/(1-z)]^{-2}$ , where  $z = p_D/p_D^{\text{max}}$  is the fraction of its maximum momentum that the  $D$  meson carries and  $\epsilon$  is a free parameter fit by using the distribution of  $z_{\text{vis}} = E_{\mu_2}/(E_{\mu_2} + E_{\text{had}})$ .

The dimuon events are divided into 5030 from incident  $\nu_{\mu}$  and 1060 from  $\bar{\nu}_{\mu}$  by assuming that the leading muon has larger transverse momentum with respect to the direction of the hadron shower than the muon from the charmed hadron decay.

Non-prompt pion and kaon decays constitute the background to the charm-initiated dimuon signal. The meson decay event generator predicts  $797 \pm 118$  events

in the identified  $\nu_\mu$ -induced sample and  $118 \pm 25$  events in the  $\bar{\nu}_\mu$  sample, based on the Lund Monte Carlo program<sup>7</sup> and test beam measurements of muon production in hadron-induced showers in the CCFR detector.<sup>8</sup>

The charm event weights are calculated using the NLO QCD charm production differential cross section calculation of Aivazis, Collins, Olness and Tung.<sup>3</sup> The calculation is performed in the  $\overline{\text{MS}}$  scheme. The factorization scale in the calculation is chosen to be  $\mu = 2p_\perp^{\text{max}}$ , where  $p_\perp^{\text{max}} = \Delta(W^2, m_c^2, M^2)/\sqrt{4W^2}$  is the maximum available transverse momentum of the initial state quark coming from the gluon splitting, or equivalently of the final state charm quark, for the given kinematic variables  $x$  and  $Q^2$ . We find the scale uncertainty by varying  $\mu$  between  $p_\perp^{\text{max}}$  and  $3p_\perp^{\text{max}}$ . The renormalization scale is chosen to equal the factorization scale. Electromagnetic radiative corrections to the cross section are calculated using the method of Bardin *et al.*<sup>9</sup>

Measurements of the  $F_2$  and  $xF_3$  structure functions by CCFR<sup>10,11</sup> are used to determine the singlet and the non-singlet quark distributions,  $xq_{SI}(x, \mu^2) = xq(x, \mu^2) + x\bar{q}(x, \mu^2)$  and  $xq_{NS}(x, \mu^2) = xq(x, \mu^2) - x\bar{q}(x, \mu^2)$ , respectively, and the gluon distribution,  $xg(x, \mu^2)$ . These distributions are obtained from next-to-leading-order QCD fits to the structure function data,<sup>12</sup> using the QCD evolution programs of Duke and Owens.<sup>13</sup>

The non-strange quark and antiquark components of the sea are assumed to be symmetric, so that  $x\bar{u}(x, \mu^2) = xu_S(x, \mu^2)$ ,  $x\bar{d}(x, \mu^2) = xd_S(x, \mu^2)$ . The strange quark content is set by the parameter

$$\kappa = \frac{\int_0^1 [xs(x, \mu^2) + x\bar{s}(x, \mu^2)] dx}{\int_0^1 [x\bar{u}(x, \mu^2) + x\bar{d}(x, \mu^2)] dx}, \quad (3)$$

where  $\kappa = 1$  would indicate a flavor SU(3) symmetric sea. The shape of the strange quark distribution relates to that of the non-strange sea by a shape parameter  $\alpha$ , where  $\alpha = 0$  would indicate that the strange sea has the same  $x$  dependence as the non-strange component of the quark sea.

#### 4. $xs(x, \mu^2) = x\bar{s}(x, \mu^2)$ fit

A  $\chi^2$  minimization is performed to find the strange sea parameters  $\kappa$  and  $\alpha$ , the values of  $B_c$  and  $m_c$ , and the fragmentation parameter  $\epsilon$ , by fitting to the  $x_{\text{vis}} = Q_{\text{vis}}^2/[2M(E_{\text{had}}^{\text{vis}} + E_{\mu_2})]$ ,  $E_{\text{vis}}$  and  $z_{\text{vis}}$  distributions of the dimuon data. Taking  $|V_{cd}| = 0.221 \pm 0.003$  and  $|V_{cs}| = 0.9743 \pm 0.0008$ <sup>14</sup> as input values and using the Collins-Spiller fragmentation function, the extracted NLO parameters with their statistical and systematic errors are presented in the first line of Table 1.

Our previous LO results,<sup>2</sup> which were found by fitting to the  $x_{\text{vis}}$  and  $E_{\text{vis}}$  distributions of the same data sample and using the Peterson fragmentation function,<sup>15</sup>  $D(z) = N\{z[1 - (1/z) - \epsilon_P/(1 - z)]^2\}^{-1}$  with  $\epsilon_P = 0.20$ , are listed in the third line of Table 1. For comparison with these results, Table 1 includes the NLO parameters determined using the same fit procedure.

Combining the NLO statistical and systematic errors in quadrature in the first error and placing the uncertainty due to QCD  $\mu^2$  scale in the second, the nucleon strange quark content is found to be  $\kappa = 0.477^{+0.051}_{-0.050}{}^{+0.017}_{+0.036}$ , indicating that the sea is not SU(3) symmetric—qualitatively the same result as from the LO analysis. The

Fit	Fragmentation	$\kappa$	$\alpha$	$B_c$	$m_c$ (GeV/c <sup>2</sup> )
NLO	Collins-Spiller $\epsilon = 0.81 \pm 0.14$	<b>0.477</b> +0.046 +0.023 -0.044 -0.024	<b>-0.02</b> +0.60 +0.28 -0.54 -0.26	<b>0.1091</b> +0.0082 +0.0063 -0.0074 -0.0051	<b>1.70</b> $\pm 0.17$ +0.09 -0.08
NLO	Peterson $\epsilon_P = 0.20 \pm 0.04$	<b>0.468</b> +0.061 +0.024 -0.046 -0.025	<b>-0.05</b> +0.46 +0.28 -0.47 -0.26	<b>0.1047</b> $\pm 0.0076$ +0.0065 -0.0052	<b>1.69</b> $\pm 0.16$ +0.12 -0.10
LO Ref.2	Peterson $\epsilon_P = 0.20 \pm 0.04$	<b>0.373</b> +0.048 -0.041 $\pm 0.018$	<b>2.50</b> +0.60 +0.36 -0.55 -0.25	<b>0.1050</b> $\pm 0.007 \pm 0.005$	<b>1.31</b> +0.20 +0.12 -0.22 -0.11

Table 1: Next-to-leading-order and leading-order fit results, assuming  $xs(x) = x\bar{s}(x)$ . Errors are statistical and systematic, except that the errors on the fragmentation parameters are statistical only.

value  $\alpha = -0.02 \stackrel{+0.66}{-0.60} \stackrel{+0.08}{-0.20}$  indicates no shape difference at NLO between  $x\bar{q}(x)$  and  $xs(x)$ . At leading order, we find the strange quarks softer than the overall quark sea by a factor  $(1-x)^\alpha$  with  $\alpha = 2.5 \pm 0.7$ . The difference in  $\alpha$  between NLO and LO is attributable to the NLO  $x\bar{q}(x)$  being softer than its LO counterpart.

The charm quark mass parameter from the NLO fit is  $1.70 \pm 0.19 \pm 0.02$ , which differs from the leading-order result, indicating a marked dependence of  $m_c$  on the order to which the analysis is done. The NLO value of  $m_c$  can be more consistently compared with measurements derived from other processes involving similar higher-order perturbative QCD calculations. A photon-gluon-fusion analysis of photoproduction data finds  $m_c = 1.74 \stackrel{+0.13}{-0.18}$ .<sup>16</sup>

### 5. $xs(x) \neq x\bar{s}(x)$ fit

Postulating intrinsic strange quark states<sup>17</sup> leads to the prediction that the  $s$  quark momentum distribution will be harder than the  $\bar{s}$  quark distribution.<sup>18</sup> We have performed a fit in which the momentum distributions of the  $s$  and  $\bar{s}$  quarks are allowed to have different shape parameters  $\alpha$  and  $\alpha'$ , respectively.

In order to reduce the number of free parameters, this fit constrains the average charmed hadron branching ratio to the value obtained from other measurements,  $B_c^1 = 0.099 \pm 0.012$  (see Section 6). We fit for  $\kappa$ ,  $\alpha$ , and  $\Delta\alpha = \alpha - \alpha'$  and the charm quark mass  $m_c$ . The result is:

$$\begin{aligned}
\kappa &= 0.536 \pm 0.030 \pm 0.036 \stackrel{-0.064}{+0.098} \pm 0.009, \\
\alpha &= -0.78 \pm 0.40 \pm 0.56 \pm 0.98 \pm 0.50, \\
\Delta\alpha &= -0.46 \pm 0.42 \pm 0.36 \pm 0.65 \pm 0.17, \\
m_c &= 1.66 \pm 0.16 \pm 0.07 \stackrel{+0.04}{-0.01} \pm 0.01 \text{ GeV}/c^2,
\end{aligned} \tag{4}$$

where the first error is statistical, the second is systematic, the third is due to the uncertainty in  $B_c^1$ , and the fourth is the error due to  $\mu^2$  scale uncertainty.

The value of  $\Delta\alpha = -0.46 \pm 0.85 \pm 0.17$  indicates that the momentum distributions of  $s$  and  $\bar{s}$  are consistent and the difference in the two distributions is limited to  $-1.9 < \Delta\alpha < 1.0$  at the 90% confidence level. This is the first quantitative comparison of the components of the  $s$  and  $\bar{s}$  quark sea.

## 6. $|V_{cd}|$ measurement

If the CKM matrix elements are not assumed, then the four parameter NLO fit in section 4 is performed by fitting  $\alpha$ ,  $m_c$  and the following products:

$$\begin{aligned} |V_{cd}|^2 B_c &= (5.34^{+0.38+0.27+0.25}_{-0.39-0.21-0.51}) \times 10^{-3}, \\ \frac{\kappa}{\kappa+2} |V_{cs}|^2 B_c &= (2.00 \pm 0.10^{+0.07+0.06}_{-0.05-0.14}) \times 10^{-2}. \end{aligned} \quad (5)$$

These combinations can be used to extract  $|V_{cd}|^2$  and  $\kappa|V_{cs}|^2$  when  $B_c$  is determined from other data.  $B_c$  is determined by combining<sup>19</sup> the charmed particle semileptonic branching ratios measured at  $e^+e^-$  colliders<sup>14</sup> with the neutrino-production fractions measured by the Fermilab E531 neutrino-emulsion experiment,<sup>5</sup> using updated values of the charmed hadron lifetimes.

We find  $B_c^I = 0.099 \pm 0.012$  and extract the value of the CKM matrix element

$$|V_{cd}| = 0.232^{+0.018}_{-0.020}, \quad (6)$$

where the error indicates all sources of uncertainty, including the  $\mu^2$  scale uncertainty. It compares very well with the PDG value,  $|V_{cd}| = 0.221 \pm 0.003$ , which is determined from measurements of the other matrix elements and the unitarity constraint on the CKM matrix assuming three generations.

## References

1. W.K. Sakumoto *et al.* (CCFR Collab.), Nucl. Inst. Meth. A 294 (1990) 179; B.J. King *et al.* (CCFR Collab.), Nucl. Inst. Meth. A 302 (1991) 254.
2. S.A. Rabinowitz *et al.* (CCFR Collab.), Phys. Rev. Lett. 70 (1993) 134.
3. M.A.G. Aivazis, J.C. Collins, F.I. Olness and W.-K. Tung, SMU-HEP/93-17.
4. R.M. Barnett, Phys. Rev. Lett. 36 (1976) 1163; H. Georgi and H.D. Politzer, Phys. Rev. D 14 (1976) 1829.
5. N. Ushida *et al.* (E531 Collab.), Phys. Lett. B 206 (1988) 375; B 206 (1988) 380.
6. P. Collins and T. Spiller, J. Phys. G 11 (1985) 1289.
7. T. Sjostrand *et al.*, Comput. Phys. Commun. 27 (1982) 243.
8. P.H. Sandler *et al.* (CCFR Collab.), Z. Phys. C 57 (1993) 1.
9. D. Bardin and N. Shumeiko, Sov. J. Nucl. Phys. 29 (1979) 499.
10. P.Z. Quintas *et al.* (CCFR Collab.), Phys. Rev. Lett. 71 (1993) 1307.
11. W.C. Leung *et al.* (CCFR Collab.), Phys. Lett. B 317 (1993) 655.
12. W.G. Seligman *et al.* (CCFR Collab.), Proc. XXVIIIth Rencontre de Moriond, ed. J. Tran Thanh Van (Editions Frontieres, Gif-sur-Yvette, 1993) p. 39.
13. D. Duke and J. Owens, Phys. Rev. D 30 (1984) 49.
14. K. Hikasa *et al.* (Particle Data Group), Phys. Rev. D 45 (1992).
15. C. Peterson *et al.*, Phys. Rev. D 27 (1983) 105.
16. J.C. Anjos *et al.* (E691 Collab.), Phys. Rev. Lett. 65 (1990) 2503.
17. S.J. Brodsky, C. Peterson and N. Sakai, Phys. Rev. D 23 (1981) 2745.
18. M. Burkardt and B.J. Warr, Phys. Rev. D 45 (1992) 958; J.D. Bjorken, priv. comm.
19. T. Bolton, Nevis Preprint R#1501.

